06

Formation of electrically conductive surfaces based on carbon nanomaterials for neurostimulation devices

© A.Yu. Gerasimenko,[1,2] A.V Kuksin,[1] D.T Murashko,[1] K.D Popovich,[1,2] U.E Kurilova,[1,2] M.S Savelyev,[1,2] I.A Suetina,[3] L.I Russu,[3] M.V Mezentseva,[3] Y.P Shaman,[1,4] E.P Kitsyuk,[1,4] I.V Nesterenko,[1,2] O.E Glukhova,[2,5] S.V Selishchev[1]

[1] Institute of Biomedical Systems, National Research University of Electronic Technology, MIET,
124498 Moscow, Zelenograd, Russian Federation
[2] Institute for Bionic Technologies and Engineering, Sechenov First Moscow State Medical University, Sechenov University,
119991 Moscow, Russia
[3] National Research Center for Epidemiology and Microbiology named after Honorary Academician N.F. Gamaleya, Ministry of Health of the Russian Federation,
123098 Moscow, Russia
[4] Scientific-Manufacturing Complex „Technological Centre“,
124498 Moscow, Russia
[5] Saratov National Research State University,
410012 Saratov, Russia
e-mail: gerasimenko@bms.zone

Received December 26, 2024
Revised December 26, 2024
Accepted December 26, 2024

The paper proposes methods for forming laser-induced carbon nanomaterials for forming electrically conductive surfaces of neuro-stimulation devices. It was found that under the action of laser radiation with an energy density in the range of $0.001-2.2\,J/cm^2$, depending on the type of nanotubes, a carbon framework structure is formed with bound carbon nanotubes and their bundles in disordered arrays of single-wall carbon nanotubes (SWCNTs) and in vertically oriented arrays of multi-wall carbon nanotubes (MWCNTs) in a bovine serum albumin (BSA) matrix and without it. For a surface based on SWCNTs in a BSA matrix, the effect of vertical orientation of nanotubes perpendicular to the surface was obtained. The specific surface area of the samples with BSA significantly decreased compared to the original nanotube arrays, however, laser exposure provided an increase of 5 and 9 times for samples based on MWCNTs and SWCNTs. Also, the addition of BSA contributed to a significant decrease in electrical conductivity, however, as a result of laser treatment, the electrical conductivity of the MWCNT array increased by 2.2 times to 0.216 kS/m, and the electrical conductivity of the disordered SWCNT array increased by 2.4 times to 0.12 kS/m. The formed surface samples provided the highest value of proliferation of nerve tissue cells compared to the control sample. For a coating of disordered SWCNT arrays in a BSA matrix, an increase in the number of cells by 24% was obtained compared to the control value after 72 hours of incubation. Thus, the formed laser-induced samples based on carbon nanotubes can be used as electrode matrices of implantable neurointerfaces for selective interaction with nerve tissue.

Keywords: carbon nanotubes, albumin, laser-induced method, electrical conductivity, electrically conductive surface, neurointerfaces, neurostimulation devices.

DOI: 10.61011/TP.2025.05.61124.453-24

Introduction

In today's world, the neuro-prosthetics and neuro-stimulation technologies are being extensively developed aimed at restoring the parts of the nervous system or modulating the pulses disrupted as a result of diseases, including neurodegenerative diseases or injuries. To control the chronic pain caused by unsuccessful spinal surgeries, angina pectoris, peripheral vascular diseases, reflex neurovascular dystrophy or phantom pain by method of stimulating the spinal cord with electrical pulses the bioelectronic devices are needed capable of receiving electricity from the nervous tissue and sending them in case of stimulation. Such nerve tissues include the brain and spinal cord, as well as areas of peripheral nerves [1]. The nervous system is responsible for transporting electrical signals that travel from the brain to the muscles to induce muscle movement and, vice versa, from the sensory organs to the brain (for example, sensations, hearing and vision). Devices that provide contact with the nervous tissue to perform diagnostic and therapeutic functions should be implantable for a long-term period of time. At the same time, to control the transmission of pain signals to the brain, such devices shall be implanted in the spinal area, and their electrode will act as a neural interface of living technical systems between a generator or receiver of electrical signals and the nervous tissue of the spinal cord [2–7]. Neural interfaces are fabricated having specific sizes and geometries, as well

as electrical and mechanical properties, to meet biological requirements in terms of their invasiveness, selectivity and performance [8,9]. For example, a beneficial topology of a neural interface is a microelectrode matrix, which is a thin layer carrying embedded conductor structures [10,11]. The dense arrangement of the charge carriers makes it possible to activate a larger number of discrete neurons or groups of neurons, which leads to increased localization and control of the desired biological response [12]. However, it is not possible to obtain microelectrode matrices with a high density of contact areas for effective stimulation of nervous tissue [13]. In most implantable devices, high-performance neural interfaces are characterized by low impedance, high electrical conductivity, and charge injection capacity for sensing and detecting, as well as safe and reversible stimulation [14].

On the one hand, in order to create effective implantable neural interfaces it is necessary to reduce their size, and on the other hand, a decrease in the conductive area is inevitably accompanied by higher impedance, and, hence, a lower signal-to-noise ratio. However, the size of the neuro-interface for clinical use is determined by a compromise between size and sensitivity [15]. Electrodes with a large geometric surface can inject a larger charge before exceeding electrochemically safe limits, however, large geometric dimensions diminish the spatial selectivity and resolution of neural interfaces [17]. In order to increase the charge injection capacity, high charge transfer capacity, and low impedance for delivery of the higher-resolution signal, it is impossible to match the specific surface area of the electrode part of the neural interface, especially given the limited space in an organ such as the spinal cord. This will allow placing a large number of electrodes to improve selectivity, accuracy and reduce the power consumption. An increase in specific surface area can be achieved using two types of neural interface modifications.

1) physical and chemical methods for providing the surface roughness;

2) methods of surface formation in deposition of films, composites, and nanomaterials with higher specific surface area and necessary electrochemical characteristics.

At the same time, the second type of modification has a greater degree of control over the structural, mechanical and electrophysical parameters of the surface due to the use of nanomaterials and their compositions with polymers [18–22].

Carbon nanomaterials can be promising materials for creating neural interfaces due to their high mechanical strength and stability sp^2 - hybridized structures with a high aspect ratio of sizes. Carbon nanomaterials have high thermal and electric conductivity and their dimensions and structure are comparable with those of the major extracellular matrix proteins [23]. External impacts from electric field, electronic beam or plasma may be used to create carcass structures with compounds that are characterized by sp^3-hybridization [24]. Laser radiation treatment can be attributed to external precision effects. Such treatment of carbon nanotube-based layers on a substrate and in the volume of a biocompatible matrix makes it possible to achieve control of their structure, mechanical and electrophysical characteristics [25–28]. For electrostimulation, it is important to deliver the charge such that to activate the action potential without affecting the cells. For this reason, it is impossible to ensure close contact between the neural interface and the nervous tissue with a mutual correspondence of structures on both sides [29]. The use of a one-dimensional carbon nanotube material with high electron mobility at high aspect ratio and surface area ensures a high level of sensitivity of bioelectronic components for measuring human electrophysiological properties during long-term monitoring [30]. Thus, carbon nanotubes may be used to form efficient neural interfaces with small areas of contact, but with high value of specific surface at low impedance and high electrical conductivity both, for the stimulating action and transmission of pulses into tissues, and for the signals readout from the tissues surface.

In view of the above, methods for the formation of electrically conductive surfaces based on carbon nanotubes and their composite materials in biopolymer matrices with a given structure and high density of charge carriers are considered in this paper, and dependences of electrical conductivity and biocompatibility on the structure and composition of the formed coatings for neural interfaces are obtained.

1. Materials and research methods

1.1. Materials used

Carbon nanotubes were used to form the electrically conductive surfaces of neuro-stimulation devices. Due to their unique electrophysical properties, nanotubes are used as active elements in functional devices and are promising materials for nanoelectronics in the form of vertically oriented, disordered arrays on a substrate or in the volume of a polymer matrix. A method that allows controlled changes in the shape, structure, and connections between nanotubes exposed to electromagnetic field of laser radiation has proven to be effective. In this regard, four types of samples of electrically conductive surfaces formed by the laser-induced method are suggested based on:

1) vertically-aligned arrays of multi-wall carbon nanotubes (MWCNT);

2) disordered arrays of single-walled carbon nanotubes (SWCNT);

3) vertically-aligned arrays of MWCNT in a polymer matrix;

4) disordered arrays of SWCNT in a polymer matrix.

Bovine serum albumin (BSA) was found suitable in fabrication of composite materials based on MWCNT and SWCNT, including biodegradable composites [31,32]. Albumin is a blood transport protein due to the presence of amino acid residues on the outer surface of its molecule;

albumin molecules have the ability to cross-link under the action of laser radiation [33].

1.2. Formation of laser-induced samples from vertically-aligned MWCNT arrays

MWCNT arrays were synthesized by method of plasma chemical vapor deposition. Heavily doped monocrystalline silicon wafers with electronic type conductivity were used as the initial substrates. Initially, a catalytic pair of metals Ti (10 nm) and Ni(2 nm) treated in Piranha solution by electron beam evaporation was deposited on the substrate. Next, the stages of oxidative and reductive annealing were carried out to form catalyst nanoparticles on the substrate. MWCNT array was synthesized using Oxford PlasmaLab System 100. The annealing was carried out at oxidation of 280 °C during 5 min in gaseous media O_2 and Ar treated by radio-frequency plasma source with a power of 100 W. The recovery was carried out at 700 °C for 5 min in the medium of gases NH_3 and Ar with treatment by radio-frequency plasma source with a power of 100 W. The average diameter of nanotubes in the sample arrays is determined mainly by the size of the formed catalyst nanoparticles on the substrate. MWCNT was $4-5\,\mu$m in length, 11–13 nm in diameter, and the number of walls varied within 8–10.

Next, a sample with a vertically-aligned MWCNT array was mounted on an optical axis perpendicular to the focused laser radiation. For laser exposure to MWCNT array, the scanning parameters were set in specialized software. An ytterbium fiber laser with wavelengths of 1064 nm, a pulse duration of 100 ns, and a pulse repetition rate of 100 kHz was used. The pulse energy varied within $1.21-4.16\,\mu$J, the pulse energy density lied within $0.4-2.2$ J/cm^2. A galvanometric scanner with two mirrors was used to position the laser beam above the sample surface. The darkened radiation was focused on the sample surface to form a laser spot with a diameter of $35\,\mu$m. When determining the irradiation trajectory, it was selected to fill the square with lines with laser dots overlapping. The degree of laser points overlapping and the speed of the beam moving along the trajectory were calculated in terms of sending the same amount of energy to a given area of MWCNT array to compensate for the intensity of the Gaussian beam profile. The lines of laser pulses had a length of 5 mm and were located parallel to each other at a distance of $17\,\mu$m. Thus, the areas of MWCNT array 10×10 mm were formed uniformly exposed to the same amount of laser radiation.

1.3. Formation of laser-induced samples from disordered SWCNT arrays

SWCNT were synthesized by the electric arc method on Ni/Y-catalytic agent, purified in the mixture of HNO_3/H_2SO_4 with further washing to obtain neutral reaction. Average diameter of nanotubes $\sim 1.4-1.8$ nm, length — $0.3-0.8\,\mu$m, specific surface — ~ 400 m^2/g. The degree of SWCNT purity was 98 %. At the first stage of samples formation, a dispersed medium of SWCNT (concentration 0.001mg/ml) and organic solvents including ethanol, isopropanol, and dimethylformamide, were used. For homogeneous distribution of SWCNT volume, the dispersed medium was treated with an immersion ultrasonic homogenizer Q700 Sonicator Qsonica at a temperature of 30–37 ° during 10 min with a specific power of 150 W/cm^2. After that, the dispersion media was treated by ultrasound Elmasonic S30H Elma with a power of 80 W during 60 min. The concentration of nanotubes was 0.001 mg/ml. At the second stage, the finished dispersed medium was applied to a silicon dioxide substrate with a size of 10×10 mm and an oxide layer thickness of $0.52\,\mu$m. The substrate was previously treated with acetone, ethanol, and distilled water in an ultrasonic bath for 5 minutes, and further was exposed to UV-radiation for 20 minutes to ensure nanotubes adhesion. The layers were applied on the substrate one by one at a temperature of 120 °C until the solvent was completely evaporated from all the applied layers. The pressure of dispersed medium supply through the 0.5 mm pneumatic nozzle was equal to 0.2 bar. A dispenser vertically mounted on a 3D movement system called E2V Nordson EFD ensured formation (due to a uniform long passage along the substrate) of a uniform layer of a disordered SWCNT system with a thickness of about the diameter of single SWCNTs and their bundles. Accordingly, to form a layer of SWCNT system $\sim 500 \pm 100$ nm thick the spray was sputtered in 500–1000 steps. At the third stage, laser exposure was used on a given area of a disordered SWCNT system in scanning mode with an energy density and radiation power of 0.061,J/cm^2 and 343,kW/cm^2, respectively. The square-shaped sample area was uniformly covered with laser spots with a diameter of $35\,\mu$m. Thus, the samples represented themselves the welded SWCNT films $0.8-1.2\,\mu$m thick on a silicon substrate.

1.4. Formation of laser-induced samples from vertically-aligned MWCNT arrays in BSA matrix

As in case of laser-induced samples from vertically-aligned MWCNT arrays, for the formation of samples from vertically-aligned MWCNT arrays in BSA matrix, MWCNTs were synthesized by plasma chemical vapor deposition on a silicon wafer under similar conditions. Next, the formed surface is placed in BSA matrix. For this purpose, a suitable suspension of distilled water and BSA with a concentration of 5 mass% by mass was prepared, a homogeneous volume distribution of which was achieved by treatment in an ultrasonic bath with a capacity of 80 W for 60 min. Instead, the finished suspension was applied on MWCNT arrays by spray deposition. In case of using BSA, the temperature of the heated table required for evaporation of the liquid components of the suspension was no higher than 50 °C in order to prevent protein denaturation that generally occurs

at higher temperatures. Complete overlapping of MWCNT arrays was achieved in 50 layers.

At the next stage of sample formation, a fast-scanning laser system was used, where a focused beam of pulsed laser radiation moved along the specified trajectory. The laser scanning pitch was $100\,\mu$m, while energy density varied from 0.001 to $0.017\,\text{J/cm}^2$. The beam moved along a square-like trajectory, with laser spots on top of each other to compensate for the intensity of the Gaussian beam profile. The scanning beam moved along the trajectory at a speed of 500 mm/s, whereas the lines of laser pulses had a length of 5 mm and were located parallel to each other at a distance of $17\,\mu$m.

1.5. Formation of laser-induced samples from disordered SWCNT arrays in BSA matrix

Initially, as described earlier, the disordered arrays of SWCNT were formed by spray deposition on a silicon substrate. For this purpose, a homogeneous dispersed medium with SWCNT concentration of 0.001mg/ml was similarly produced, which was applied in layers to a heated substrate using a spray system in order to form a stable layer of disordered SWCNT nets with a thickness of $\sim 500 \pm 100$nm.

Next, the prepared system was placed in BSA matrix by spray deposition of the homogeneous polymer suspension with a concentration of 5,mass

1.6. Studying the structure and conductivity of samples

The structural characteristics of the samples on silicon wafers were studied by method of scanning electron microscopy (SEM) using device FEI Helios NanoLab 650. The value of the accelerating voltage of the electron column was set at 5 kV for SWCNT and SWCNT arrays, and the current of the electron probe was 50 pA. For BSA coated samples the accelerating voltage and current were set at levels 1 kV and 25 pA, respectively. The pressure in the chamber was maintained at $3.9 \cdot 10^{-4}$ Pa. The samples were fixed on a conductive substrate using carbon ribbon.

By using the method of low-temperature nitrogen porosity measurement via „Sorptometer-M" Katacon system the specific surface of nanomaterials was studied. The samples were degassed and cooled to a temperature of 77 K in liquid nitrogen. Next, nitrogen was adsorbed on the sample surface. The proportion of nitrogen increased until a partial pressure close to saturated was reached. After that, the sample was heated and nitrogen was desorbed from the sample surface. The volume fraction of nitrogen in the mixture was detected using a thermal conductivity detector. The output operating signal of the detector was a peak of increased nitrogen concentration converted into an electrical signal during its thermal desorption from the sample surface. The area of this peak is proportional to the volume of nitrogen desorbed from the sample surface. After partial pressure was reached, the desorption isotherm was plotted. To plot the desorption isotherm, the sample was saturated with nitrogen again, while the composition of the gas medium changed and the amount of desorbed nitrogen was measured. The specific surface area of samples was calculated using method of Barrett-Joyner-Halenda (BJH) [34].

To determine the electrical conductivity of films, the Van der Pauw four-probe method was chosen, which makes it possible to measure the resistivity of films with high accuracy [35]. The nanomaterials in film form on the substrate were given a square shape, and measurements were carried out using Cascade Microtech PM5 platinum pointed probes connected to a two-channel precision parametric analyzer Keysight B2912A.

1.7. Biocompatibility studies

Studies of the compatibility of the obtained samples with cells were carried out on the Neuro2a nerve tissue cell culture provided by the N.F.Gamalei National Research Center for Epidemiology and Microbiology. Two types of studies were performed — cell survival assessment by MTS assay and fluorescence microscopy for a more detailed analysis of cell morphology and cell distribution over the sample surface. For each of the studies, the samples were placed on the bottom of a culture plate and filled with a cell suspension in amount of $3 \cdot 10^5$ cell/ml. Further, the plates were placed in CO_2-thermostat for 72 h, upon completion of this period the MTS assay was made. The other part of the samples was stained with Hoeschst 33342 dye after 72 h of incubation with cells and examined using Olympus fv3000 confocal laser scanning microscope.

2. Results and discussion

2.1. Investigation of the structural features of electrically conductive surfaces based on carbon nanomaterials

As a result, four types of samples of electrical-conductive surfaces were formed by the laser-induced method based on:

1) vertically-aligned arrays of MWCNT;
2) disordered arrays of SWCNT;
3) vertically-aligned arrays of MWCNT in BSA matrix;
4) disordered arrays of SWCNT in BSA matrix.

Fig. 1 shows SEM image of initial vertically-aligned MWCNT array (Fig. 1, *a, b*) and MWCNT array after laser exposure (Fig. 1, *c, d*).

As can be seen from the SEM image (Fig. 1, *c, d*), after synthesis, the MWCNT in the array did not look sufficiently straightened, the upper ends of the nanotubes were randomly oriented. After synthesis, the MWCNT arrays were exposed to laser radiation in the scanning mode with the parameters described above. As can be seen from the SEM image (Fig. 1, *c, d*), as a result of

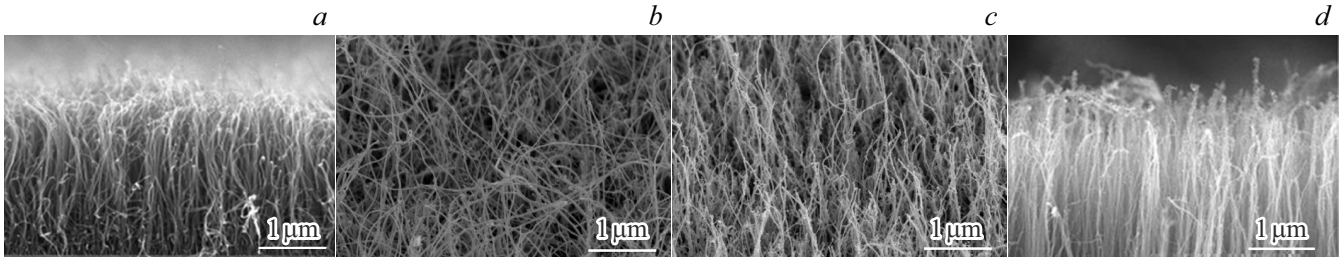

Figure 1. Vertically-aligned MWCNT arrays on a silicon substrate in the original form (a, b) and after laser exposure (c, d).

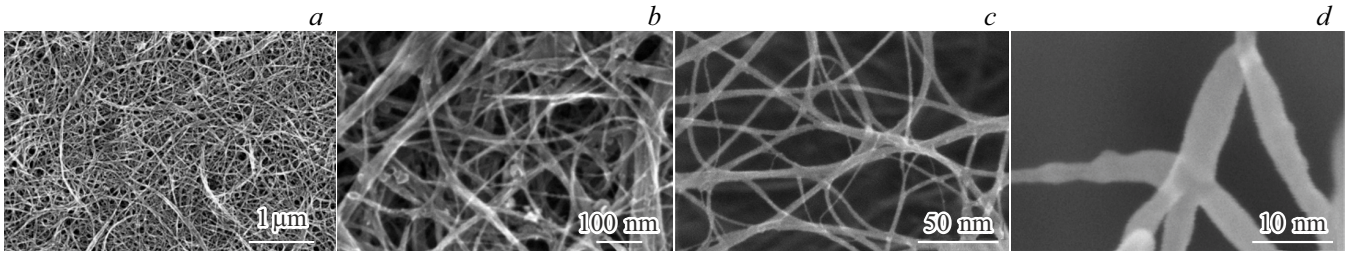

Figure 2. Disordered SWCNT arrays on silicon substrate in its original form (a, b) and after exposure to laser radiation (c, d).

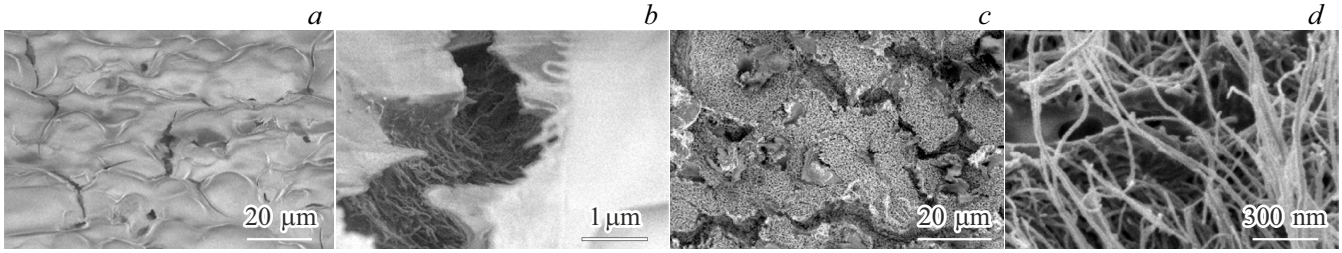

Figure 3. Vertically-aligned MWCNT arrays in BSA matrix on a silicon substrate in the original form (a, b) and after laser exposure (c, d).

laser exposure, the MWCNT became vertically oriented relative to the substrate. Some of the sublimated carbon inclusions were deposited on the surface of the nanotube array after laser exposure. The upper ends of MWCNT were connected to each other, thus new channels were formed that provide more efficient electron transport compared to the original MWCNT array. The nanotubes were bonded by forming covalent bonds between defective sections of the outer layers of neighboring nanotubes, as well as by forming solder as an amorphous carbon, which is formed as a result of sublimation of defective open ends of MWCNT under laser exposure.

The next step was to form disordered arrays of SWCNT on the substrates. Fig. 2, *a, b* illustrates SEM images of the surface of SWCNT array after being applied on the substrate.

In the initial array, there were both individual SWCNT and their bundles, the diameter of which reached 40 nm. As a result of the laser effect on SWCNT array the effect of binding the SWCNT and their bundles to form an extensive network was achieved (Fig. 2, *c, d*). In places of the intersecting and perpendicular arrangement of the tubes, connections of SWCNT with X-, T- and Y-shapes were formed. It can be seen from the obtained SEM images that almost all areas of SWCNT binding to each other have a color similar to the color of the rest of the nanotube surface. This may be due to the uniform discharge of charge from the entire SWCNT network due to the same electrical conductivity.

Next, the structure of the electrically conductive surface of vertically-aligned MWCNT arrays in BSA matrix was analyzed using SEM method before and after laser exposure with an energy density in the range of $0.001-0.017\,\mathrm{J/cm^2}$ (Fig. 3).

On SEM images of MWCNT array covered with a layer of BSA (before laser exposure)? the nanotubes are not seen (Fig. 3, *a*). The surface of the biopolymer was characterized by rare cracks up to $30\,\mu$m in size, where the presence of MWCNT was detected, however, the nanotubes in the area of contact with the biopolymer had a chaotic orientation (Fig. 3, *b*). Vertical deposition of a sprayed BSA suspension directed perpendicular to the substrate led to a change in the distance between MWCNT and manifestation of bond energy between individual nanotubes. As a result, the

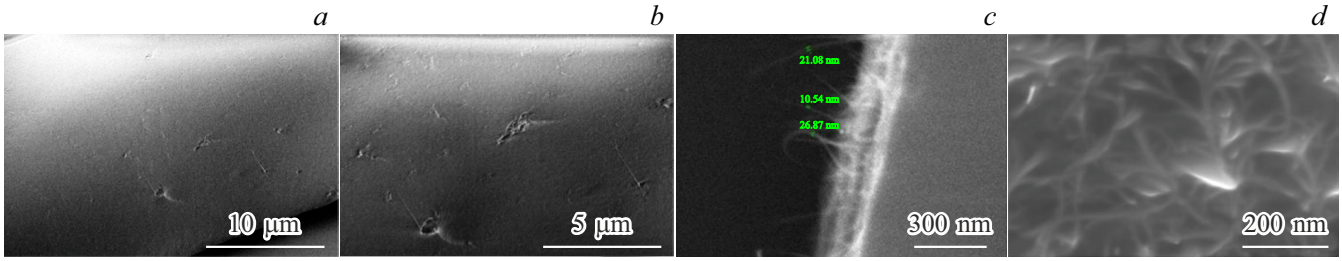

Figure 4. Disordered SWCNT arrays in BSA matrix on silicon substrate in its original form (a, b) and after exposure to laser radiation (c, d).

Table 1. Specific surface area of carbon nanotube-based samples

Type of sample	Specific surface area initial samples, m^2/g	Specific surface area of laser-induced samples, m^2/g
Vertically-aligned MWCNT arrays	310 ± 15	245 ± 8
Disordered SWCNT arrays	435 ± 20	320 ± 15
Vertically-aligned MWCNT arrays in BSA matrix	7 ± 0.5	36 ± 4
Disordered SWCNT arrays in BSA matrix	3 ± 0.2	27 ± 1.3

nanotubes were reoriented, as well as their intertwining and, in some cases, the formation of bundles.

In the process of laser exposure with an energy density of more than $0.001 J/cm^2$, the energy is absorbed by electrons and converted into atomic energy. The collision of phonons with carbon atoms leads to the formation of defects such as vacancies and internodes in the main chain of nanotubes, which leads to the rupture and formation of new C–C bonds in various layers of MWCNT. Chemical bonds are formed on the contact surface of bonded carbon nanotubes. This causes reconstruction of graphene layer surfaces and reduction of their diameter. In the region of the outer graphene layer, MWCNT compounds are formed, which ensures welding with the formation of pairs of seven- and pentagons of carbon atoms [36–38]. 3, *c, d* shows that when exposed to laser radiation, the amount of BSA on the sample surface decreased, and the synthesized vertically-aligned MWCNT arrays changed their morphology, on the one hand, due to bending, on the other hand, when binding to each other, forming an electrically conductive network. Thus, when laser radiation is applied to the surface of vertically-aligned MWCNT arrays, X-, Y-, and T-shaped junctions between nanotubes are formed in BSA matrix, which form a cellular structure in the polymer matrix. Additionally, it was possible to confirm the envelopment of this network with a polymer layer, as the diameter of the nanotubes increased by 20–40 %. Further increase in the energy density to values exceeding $0.017 J/cm^2$ led to the destruction of the sample structure associated with carbon sublimation.

The structure of the electrically conductive surface of disordered SWCNT arrays in BSA matrix in its original form and after laser exposure was studied in a similar way (Fig. 4).

The obtained SEM images made it possible to characterize the initial surface before using the laser-induced method as smoother and more uniform surface, without visible cracks (Fig. 4, *a, b*). As in case of vertically-aligned MWCNT arrays in BSA matrix, after exposure to laser radiation, part of the polymer layer was removed, and therefore in Fig. 4, *c,* d it can be attributed to MWCNT system, the diameter of which was also increased by 20–40 % due to the coating of their external structure with a layer of BSA. In addition, it has also been established that laser exposure with an energy density in the range of $0.001–0.017 J/cm^2$ ensures the structuring of MWCNT in BSA matrix due to their binding to each other at the sites of defects. At the same time, after laser exposure caused by the binding of nanotubes to each other, the effect of vertical alignment of SWCNT and their bundles in the albumin matrix was observed on the sample surface. At a lower energy density, the nanotubes did not bind, and at a higher energy density, the structure collapsed.

The study of the structural features and specific surface area in combination with electrical conductivity of the fabricated carbon nanotubes made it possible to identify their applicability as contact pads for the implantable neural-interface electrode matrix. Isolated SWCNT have the largest external specific surface area, the value of which reaches $\sim 1300 m^2/g$. However, when bundles of two,

Table 2. Conductivity of carbon nanotube-based samples

Type of sample	Electric conductivity initial samples, kS/m	Electric conductivity of laser- of laser-induced samples, kS/m
Vertically-aligned MWCNT arrays	0.8 ± 0.06	52 ± 9
Disordered arrays of SWCNT	2.3 ± 0.18	980 ± 43
Vertically-aligned MWCNT arrays in BSA matrix	0.1 ± 0.006	0.216 ± 0.015
Disordered arrays of SWCNT in BSA matrix	0.05 ± 0.004	0.12 ± 0.016

three, or more nanotubes are formed under the action of Van der Waals forces, the specific surface area decreases to $200-400\,m^2/g$. At the same time, the values of the specific surface area of the isolated MWCNT reach lower values than SWCNT, due to the lower aspect ratio. In the vertically-aligned MWCNT array, the value of the specific surface area depends, in addition to the morphological features of individual nanotubes, on the density of the array, which is determined by the density of formation of catalytic particles during the synthesis of nanotubes. Table 1 shows the specific surface area values of the obtained types of samples based on MWCNT and SWCNT carbon nanomaterials, as well as nanotubes in the albumin matrix. 5 measurements were carried out for each sample, after which the average values and errors were calculated.

It was found that initial samples of MWCNT and SWCNT arrays were characterized by the highest specific surface area that made (310 ± 15) and $(435 \pm 20)\,m^2/g$ respectively, while specific surface area for the laser-induced MWCNT and SWCNT samples declined, respectively, by 21 and 27 %. This may be due to the formation of a carbon skeleton material from nanotubes and their bundles, characterized by the presence of large-sized structural elements after laser exposure. The BSA coating of vertically-aligned MWCNT arrays and disordered SWCNT arrays led to a sharp decrease in the specific surface area by 44 and 145 times, respectively. However, laser exposure ensured the removal of the surface part of the BSA and the formation of a skeleton structure combined with an albumin layer. The specific surface area of such layers increased by 5 and 9 times for MWCNT-based and SWCNT-based samples.

2.2. Studies of electrically conductive surfaces based on carbon nanomaterials

A four-probe method was used to measure the electrical conductivity of the formed initial and laser-induced samples. The electrical conductivity of each sample was recorded at five points, after which the average values of electrical conductivity and errors were calculated. The measurement results are presented in Table 2.

It can be seen from the results obtained that the laser effect on the vertically-aligned MWCNT array led to a 65-fold increase in electrical conductivity (52 ± 9) kS/m. The initial disordered SWCNT array had electrical conductivity of (2.3 ± 0.18) kS/m. At the same time, laser treatment led to a 426-fold increase in electrical conductivity up to (980 ± 43) kS/m. The vertically-aligned MWCNT array and the disordered SWCNT array in BSA matrix had lower electrical conductivity values — (0.1 ± 0.007) kS/m and (0.05 ± 0.004) kS/m, respectively. As a result of laser treatment, the electrical conductivity of MWCNT array increased by 2.2 times to (0.216 ± 0.015) kS/m, and the conductivity of disordered SWCNT array increased by 2.4 times to (0.12 ± 0.016) kS/M. For all samples, laser exposure leads to an increase in electrical conductivity, which indicates the formation of bonds between carbon nanotubes and their bundles both in BSA matrix and without it.

Thus, vertically-aligned MWCNT arrays, including MWCNT arrays in BSA matrix and laser-induced SWCNT arrays with BSA can provide high charge transfer capability due to high values of specific surface area, aspect ratio, electrical conductivity, as well as high field gain and stable current density. Such properties of the obtained electrically conductive surfaces based on laser-induced carbon nanomaterials can be effective for stimulating nerve tissues due to the low impedance in sending electrical signal with a higher resolution of the location of the neural interface conductive domains by enlarging the specific surface area, which allows placing a large number of electrodes to increase selectivity, accuracy and reduce energy consumption, especially during implantation of the neural interface in the spinal cord.

2.3. Biocompatibility of surfaces based on carbon nanomaterials

For an initial assessment of the biocompatibility of the formed coatings based on carbon nanomaterials, studies using Neuro2a type nerve cells were conducted. Laser-induced samples with high electrical conductivity values were selected for cellular studies. Based on the results of MTS assay, a curve of optical density versus sample composition was plotted (Fig. 5). The optical density of

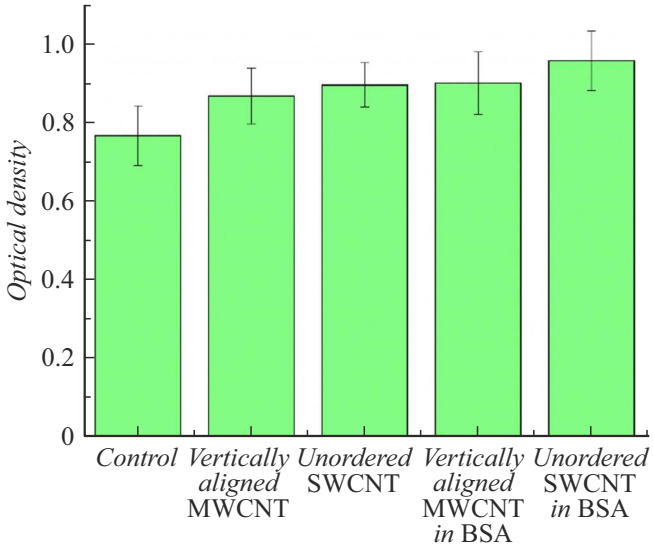

Figure 5. Results of the MTS assay of laser-induced samples based on carbon nanotubes.

the cell suspension in the empty well of the culture plate acts as a control. The curve shows that for all samples, the cells survival rate exceeds the control value, while the best results are observed for samples from disordered SWCNT arrays in BSA matrix. In this case, the presence of a biopolymer has a positive effect on cell survival, while for single-walled nanotubes, we can talk about more efficient polymer wrapping.

For fluorescence microscopy studies, a pure silicon wafer without a sample was used as a control. In the experimental samples, the cells are more evenly distributed over the surface, their number exceeds the number of cells in the control, which is consistent with the MTS assay data. At the same time, the cytomorphology is preserved, which indicates the absence of toxicity of the studied materials. (Fig. 6).

It was found that for the SWCNT-based sample, the largest number of nerve tissue cells was obtained in BSA matrix after 72 h incubation, which is 24% more than the control value. The conducted biocompatibility studies indicate the possibility of using laser-induced carbon nanotube samples as contact pads for the implantable neural interfaces.

Conclusion

In this paper, methods for the formation of laser-induced carbon nanomaterials for creating electrically conductive surfaces of neuro-stimulation devices are proposed. As a result the surfaces were formed based on the vertically-aligned MWCNT arrays, disordered SWCNT arrays, as well as vertically-aligned MWCNT arrays and disordered SWCNT arrays in BSA matrix. It has been found that under the action of laser radiation with an energy density in the range of $0.001-0.4\,\mathrm{J/cm^2}$, a carbon skeleton structure is formed with bound carbon nanotubes and their bundles in disordered and vertically-aligned arrays on the substrate and

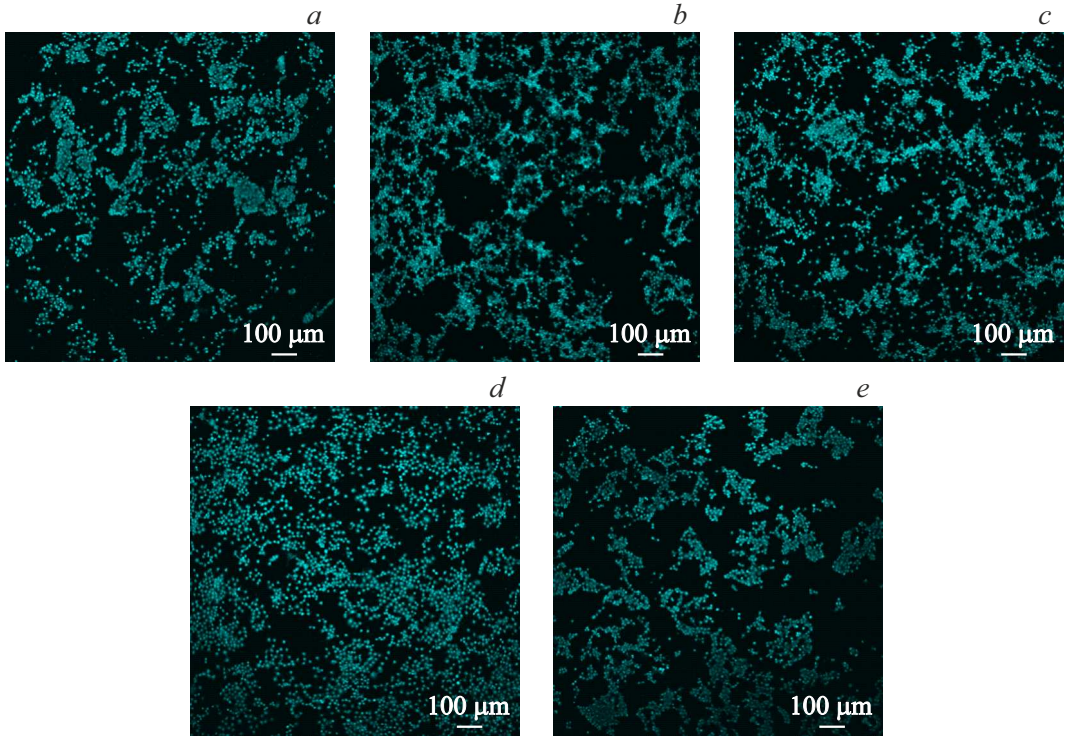

Figure 6. Fluorescence microscopy of laser-induced carbon nanotube samples: vertically-aligned MWCNT arrays (a), disordered SWCNT arrays (b), vertically-aligned MWCNT arrays in BSA matrix (c), disordered SWCNT arrays in polymer matrix (d), control sample (e).

in BSA matrix. The effect of vertically-aligned nanotubes perpendicular to the surface was obtained for a SWCNT-surface in BSA matrix. It was found that the specific surface area of laser-induced MWCNT-based and SWCNT-based samples decreased by 21 and 27%, respectively, which may be due to the formation of a carbon skeleton material from nanotubes and their beams, characterized by the presence of large-sized structural elements after laser radiation. However, laser exposure ensured the removal of the surface part of the BSA and the formation of a skeleton structure combined with an albumin layer. The specific surface area of such layers increased by 5 and 9 times for MWCNT-based and SWCNT-based samples. The laser radiation was found to increase the conductivity of vertically-aligned MWCNT arrays by 65 times up to 52 kS/m, and for the disordered SWCNT arrays by 426 times up to 980 kS/m. After BSA had been added to the carbon nanomaterials it contributed to significant decrease in conductivity, however after laser treatment the conductivity of MWCNT array grew by 2.2 times up to 0.216 kS/m, whereas conductivity of the disordered SWCNT array increased by 2.4 times up to 0.12 kS/m. Thus, arrays of vertically-aligned MWCNT, including MWCNT arrays in BSA matrix and laser-induced SWCNT arrays with BSA can be highly capable of transferring the charge to nerve tissues when high-resolution implantable neural interface electrode arrays for the target interaction with nervous tissue are fabricated of them. For this purpose, studies were conducted using nerve tissue cells, which showed an excess of cells survival on surfaces made of carbon nanomaterials compared with the control sample. The highest cells proliferation was obtained for the disordered SWCNT arrays in BSA matrix (by 24% times higher compared to the control value). In this case, the presence of a biopolymer has positive effect on cell survival. The conducted biocompatibility studies indicate the possibility of using laser-induced carbon nanotube samples as contact pads for the implantable neural interfaces.

Funding

This study was performed as part of a large research project and funded by the Russian Federation represented by the Ministry of Science and Higher Education of the Russian Federation under Agreement № 075-15-2024-555 dated April 25, 2024.

Conflict of interest

The authors declare that they have no conflict of interest.

References

[1] L.J. Epstein, M. Palmieri. Mount Sinai J. Medicine: A. J. Translational and Personalized Medicine, **79** (1), 123 (2012). DOI: 10.1002/msj.21289

[2] L. Theogarajan. Neuroscience Lett., **519** (2), 129 (2012). DOI: 10.1016/j.neulet.2012.02.001

[3] S.K. Kelly, D.B. Shire, J. Chen, P. Doyle, M.D. Gingerich, S.F. Cogan, W.A. Drohan, S. Behan, L. Theogarajan, J.L. Wyatt, J.F. Rizzo III. IEEE Transactions on Biomed. Eng., **58** (11), 3197 (2011). DOI: 10.1109/TBME.2011.2165713

[4] M.L. Carlson, C.L. Driscoll, R.H. Gifford, S.O. McMenomey. Otolaryngologic Clinics of North America, **45** (1), 221 (2012). DOI: 10.1016/j.otc.2011.09.002

[5] T. Wolter. J. Pain Res., **2014** (7), 651 (2014). DOI: 10.2147/jpr.S37589

[6] K.M. Alo, J. Holsheimer. Neurosurgery, **50** (4), 690 (2002). DOI: 10.1097/00006123-200204000-00003

[7] R. Melzack, P.D. Wall. Science, **150** (3699), 971 (1965). DOI: 10.1126/science.150.3699.971

[8] C. Boehler, T. Stieglitz, M. Asplund. Biomaterials, **67**, 346 (2015). DOI: 10.1016/j.biomaterials.2015.07.036

[9] K. Bradley. Pain Medicine, **7** (suppl_1), S27 (2006). DOI: 10.1111/j.1526-4637.2006.00120.x

[10] R.A. Normann, E. Fernandez. J. Neural Eng., **13** (6), 061003 (2016). DOI: 10.1088/1741-2560/13/6/061003

[11] C.J. Hayden, C. Dalton. Appl. Surf. Sci., **256** (12), 3761 (2010). DOI: 10.1016/j.apsusc.2010.01.022

[12] H. Cagnan, T. Denison, C. McIntyre, P. Brown. Nature Biotechnol., **37** (9), 1024 (2019). DOI: 10.1038/s41587-019-0244-6

[13] R.A. Green, N.H. Lovell, G.G. Wallace, L.A. Poole-Warren. Biomaterials, **29** (24–25), 3393 (2008). DOI: 10.1016/j.biomaterials.2008.04.047

[14] P. Daubinger, J. Kieninger, T. Unmüssig, G. A. Urban. Phys. Chem. Chem. Phys., **16** (18), 8392 (2014). DOI: 10.1039/c4cp00342j

[15] C. Boehler, T. Stieglitz, M. Asplund. Biomaterials, **67**, 346 (2015). DOI: 10.1016/j.biomaterials.2015.07.036

[16] S.F. Cogan. Annu. Rev. Biomed. Eng., **10** (1), 275 (2008). DOI: 10.1146/annurev.bioeng.10.061807.160518

[17] R.A. Green, P.B. Matteucci, C.W.D. Dodds, J. Palmer, W.F. Dueck, R.T. Hassarati, P.J. Byrnes-Preston, N.H. Lovell, G.J. Suaning. J. Neural Eng., **11** (5), 056017 (2014). DOI: 10.1088/1741-2560/11/5/056017

[18] E. Ben-Jacob, Y. Hanein. J. Mater. Chem., **18** (43), 5181 (2008). DOI: 10.1039/b805878b

[19] N. Driscoll, K. Maleski, A.G. Richardson, B. Murphy, B. Anasori, T.H. Lucas, Y. Gogotsi, F. Vitale. J. Visualized Experiments, **156**, e60741 (2020). DOI: 10.3791/60741

[20] T. Latif, M. McKnight, M.D. Dickey, A. Bozkurt. PLoS One, **13** (10), e0203880 (2018). DOI: 10.1371/journal.pone.0203880

[21] R. Green, M.R. Abidian. Adv. Mater., **27** (46), 7620 (2015). DOI: 10.1002/adma.201501810

[22] S.K. Seidlits, J.Y. Lee, C.E. Schmidt. Nanomedicine, **3** (2), 183 (2008). DOI: 10.2217/17435889.3.2.183

[23] S.H. Ku, M. Lee, C.B. Park. Adv. Healthcare Mater., **2** (2), 244 (2013). DOI: 10.1002/adhm.201200307

[24] J. Kim, G.G. Kim, S. Kim, W. Jung. Appl. Phys. Lett., **108**, 203110 (2016). DOI: 10.1063/1.4952397

[25] A.Y. Gerasimenko, A.V. Kuksin, Y.P. Shaman, E.P. Kitsyuk, Y.O. Fedorova, D.T. Murashko, A.A. Shamanaev, E.M. Eganova, A.V. Sysa, M.S. Savelyev, D.V. Telyshev, A.A. Pavlov, O.E. Glukhova. Nanomaterials, **12** (16), 2812 (2022). DOI: 10.3390/nano12162812

[26] A.Y. Gerasimenko, A.V. Kuksin, Y.P. Shaman, E.P. Kitsyuk, Y.O. Fedorova, A.V. Sysa, A.A. Pavlov, O.E. Glukhova. Nanomaterials, **11**, 1875 (2021). DOI: 10.3390/NANO11081875
[27] A.Y. Gerasimenko, G.N. Ten, D.I. Ryabkin, N.E. Shcherbakova, E.A. Morozova, L.P. Ichkitidze. Spectrochim. Acta Part A Mol. Biomol. Spectrosc., **227**, 117682 (2020). DOI: 10.1016/j.saa.2019.117682
[28] A.Y. Gerasimenko, U.E. Kurilova, M.S. Savelyev, D.T. Murashko, O.E. Glukhova. Compos. Struct., **260**, 113517 (2021). DOI: 10.1016/j.compstruct.2020.113517
[29] B.C. Kang, T.J. Ha. Jpn. J. Appl. Phys., **57** (5S), 05GD02 (2018), DOI: 10.7567/JJAP.57.05GD02
[30] Q.L. Zhao, Z.M. Wang, J.H. Chen, S.Q. Liu, Y.K. Wang, M.Y. Zhang, J.-J. Di, G.-P. He, L. Zhao, T.-T. Su, J. Zhang, X. Liang, W.-L. Song, Z.L. Hou. Nanoscale, **13** (24), 10798 (2021). DOI: 10.1039/D0NR08032B
[31] A.Y. Gerasimenko, G.N. Ten, D.I. Ryabkin, N.E. Shcherbakova, E.A. Morozova, L.P. Ichkitidze. Spectrochim. Acta Part A Mol. Biomol. Spectrosc., **227**, 117682 (2020). DOI: 10.1016/j.saa.2019.117682
[32] A.Y. Gerasimenko, U.E. Kurilova, M.S. Savelyev, D.T. Murashko, O.E. Glukhova. Compos. Struct., **260**, 113517 (2021). DOI: 10.1016/j.compstruct.2020.113517
[33] Z. Han, H. Kong, J. Meng, C. Wang, S. Xie, H. Xu. J. Nanosci. Nanotechnol., **9** (2), 1400 (2009). DOI: 10.1166/jnn.2009.C165
[34] E.P. Barrett, L.G. Joyner, P.P. Halenda. J. American Chem. Society, **73** (1), 373 (1951). DOI: 10.1021/ja01145a126
[35] L.P. Ichkitidze, A.Y. Gerasimenko, V.M. Podgaetsky, S.V. Selishchev, A.A. Dudin, A.A. Pavlov. Mater. Phys. Mechan., **37** (2), 140 (2018).
[36] A.V. Krasheninnikov, K. Nordlund, M. Sirviö, E. Salonen, J. Keinone. Phys. Rev. B, **63** (24), 245405 (2001).
[37] A.Y. Gerasimenko, O.E. Glukhova, G.V. Savostyanov, V.M. Podgaetsky. J. Biomed. Opt., **22** (6), 065003 (2017).
[38] A.Y. Gerasimenko, A.V. Kuksin, Y.P. Shaman, E.P. Kitsyuk, Y.O. Fedorova, A.V. Sysa, A.A. Pavlov, O.E. Glukhova. Nanomaterials, **11**, 1875 (2021).

Translated by T.Zorina